Florian Krainer, BSc

Validation of an Oxygen Measuring System for Industrial Scale Bioreactors to Investigate Local Oxygen Transfer Rates

MASTER'S THESIS

to achieve the university degree of

Diplom-Ingenieur

Master's degree programme: Chemical and Process Engineering

submitted to

Graz University of Technology

Supervisor

Assoc. Prof. Dipl.-Ing. Dr. techn. Stefan Radl

Institute of Process & Particle Engineering

Graz, October 2018

AFFIDAVIT

I declare that I have authored this thesis independently, that I have not used other than the declared sources/resources, and that I have explicitly indicated all material which has been quoted either literally or by content from the sources used. The text document uploaded to TUGRAZonline is identical to the present master‘s thesis dissertation.

Date

Signature

Copyright

Danksagung

An dieser Stelle möchte ich mich bei meinem Betreuer Assoc.Prof. Dr. Stefan Radl für die umfangreiche und unkomplizierte Betreuung, Korrektur und Optimierung meiner Arbeit bedanken.

Einen Dank möchte ich auch meinen Vorgesetzten und meinen Kollegen der Firma ZETA aussprechen, die es mir möglich machten Studium und Arbeit zu kombinieren und vor allem in beiden Bereichen Freude zu bewahren.

Die Messmethodik dieser Arbeit entsprang einer simplen Idee und schaffte es schließlich zur ACHEMA 2018, wo ich sie selbst präsentieren durfte. Das war möglich durch Risikobereitschaft und Vertrauen der Geschäftsführung der Firma ZETA, daher noch ein besonderer Dank und auf eine gute weitere Zusammenarbeit!

Selbstverständlich möchte ich an dieser Stelle auch bei meinen Eltern bedanken, die mich mein ganzes Studium begleitet und unterstützt haben.

Ein großer Dank gilt auch meiner Freundin Ulli, die immer an meiner Seite ist und mich motiviert hat, wenn es zwischendurch nötig war.

Table of Contents

Abbreviations

DSM	Dynamic step method
DPM	Dynamic pressure method
FDA	Food and drug administration
GMP	Good manufacturing practice
STR	Stirred tank reactor

Nomenclature

Latin Symbols

a	Liquid exchange area per liquid volume	[m²/m³]
C	Oxygen concentration	[g/L] or [%]
C^*	Saturation concentration	[g/L] or [%]
C_{me}	Measured concentration	[g/L] or [%]
D	Diameter	[m]
D_{eff}	Diffusion coefficient	[m²/s]
H^{cp}	Henry constant	[m^{-3} Pa^{-1}]
k_L	Mas transfer coefficient	[m/s]
k_La	Volumetric oxygen mass transfer coefficient	[1/s]
k_La^*	Local oxygen supply rate	[1/s]
l	Length	[m]
OTR	Oxygen transfer rate	[g L^{-1} s^{-1}]
OUR	Oxygen update rate	[g L^{-1} s^{-1}]
p	Pressure	[Pa]
P_g	Power input	[W]
Re	Reynolds number	[-]
t	Time	[s]
V_L	Filling Volume	[m³]
ν	Kinematic viscosity	[m²/s]
vvm	Gassing volume per vessel volume per minute	[1/min]

Greek Symbols

τ_r	Reaction time	[s]
ϑ	Velocity	[m/s]
ϑ_S	superficial air velocity	[m/s]
ζ	Pressure loss coefficient	[-]
μ	specific growth rate	[1/h]

Abstract

Within this thesis, different methods to measure the volumetric oxygen mass transfer coefficient (i.e. k_La) in a Stirred Tank Reactor (STR) are compared with specific focus on their usability in industrial plants. The Dynamic Pressure Method (DPM) and the Dynamic Step Method (DSM) become apparent to be the most suitable one. Furthermore, a new measuring method that is based on a flow through cell is introduced and compared to a standard sensor. It is capable to measure the oxygen concentration at any position inside the STR without being disturbed by the gas phase. It is shown, that the new measuring method does not have a negative influence on the system compared to a standard sensor.
With the new method, the DSM is used to estimate mass transfer coefficients from data collected at different positions of a 20L and a 150L STR. The results show that the two systems, although they have the same design parameters, cannot be described with the same model equations.

Zusammenfassung

Im Rahmen dieser Arbeit werden verschiedene Methoden zur Bestimmung des volumenbezogenen Stoffübergangskoeffizienten in Bioreaktoren mit besonderem Augenmerk auf ihre Einsatzfähigkeit in Produktionsanlagen verglichen. Es zeigt sich, dass die dynamische Druckänderungsmethode (DPM) und die dynamische Schrittmethode (DSM) am besten geeignet sind. Desweitern wird eine neue Messmethode, die mittels Durchflusszelle den Sauerstoffgehalt an jeder Position im Reaktor messen kann, vorgestellt. Diese wird mit einem Standardsensor verglichen, um zu beweisen, dass sie durch ihre Methodik keinen negativen Einfluss auf das System hat.
Ein 20L und ein 150L Reaktor werden anschließend mit der neuen Messmethode und der DSM an verschieden Punkten hinsichtlich ihrer Stoffaustauschcharakteristik vermessen.
Dabei zeigt sich, dass die zwei Systeme, obwohl sie die gleichen Auslegungsparameter haben, nicht mit denselben Modellgleichungen beschrieben werden können.

1. Introduction

The fast development of new biopharmaceutical drugs affects many industries and acts as driving force for new components and a better process understanding. Particular importance has to be given to the fermentation process, since it is the key production step for many biopharmaceutical products[1]. The challenge in optimizing a process with living organisms is that (i) these microorganisms have highly specific nutrient requirements, that (ii) the influence of the process parameters on the microorganisms are hard to predict, and that (iii) these parameters often cannot be determined individually. Statistical approaches are often used to investigate correlations between process parameters and the performance of the cells (e.g. growth rate and product yield) [2].

Besides creating an appropriate biosphere (e.g., temperature, pH, pressure), an optimal supply of nutrients is the key to a good fermentation process. Oxygen, as a nutrition, needs a special consideration, since it gets supplied in the gas phase and has to dissolve in the liquid phase before it can be metabolized by microorganisms [3].

1.1. Motivation

The present thesis will focus on the oxygen transfer rate (OTR) in aerobic fermentation processes, particularly the measurement of the volumetric oxygen mass transfer coefficient (k_La) in a Stirred Tank bio-Reactor (STR) and the influence of its design.

For the financing industrial partner (i.e., ZETA Holding GmbH) the present thesis will provide the tools for a better process understanding regarding the design and operating conditions of STRs. Also, a new service for customers, where an existing bioreactor is characterized regarding its oxygen transfer rate, will be possible with the methods discussed in this thesis. With such a characterization a customer (i) gains process know how, (ii) is able to optimize the system parameters, and (iii) can compare different bioreactors or production plants. All these possibilities are of high value to operators of industrial fermentation plants, motivating the present thesis.

1.2. Goals

The primary goal of the present thesis is to show the usability of a new measuring method, especially for the usage at an industrial plant with all the limitations and requirements that apply to such a scale (e.g., the application in a clean room, the limitation on only using validated media components, and impossibility of constructional changes)

Specific sub-goals are:

- Investigation of the influence of gas bubbles on the measurement result
- Quantification of the dependence of the k_La on the measuring position
- Collection of results of the k_La for a reactor scale up study

1.3. Outline

Chapter 2 gives a short definition of the fermentation process and shows its history and why the oxygen transfer rate is of major importance for any aerobic process.

The background in the field of oxygen transfer rate measurements is summarize in the Chapters 3 to 4. A new oxygen measurement procedure with a flow through cell is presented, and compared to standard oxygen sensors (see Chapter 0). Thereby, the focus is on demonstrating the advantages of the newly developed flow through cell regarding the accuracy and flexibility of the measurement (see results presented in Chapter 6.3). Particularly, with the new measuring method it is possible to pay focus on the local distribution of the k_La inside an STR, and so zones with high and low OTR can be identified (see the demonstration in Chapter **Fehler! Verweisquelle konnte nicht gefunden werden.**). The usage of the method is demonstrated with two STR (i.e., 20L and 150L) and the challenges of a k_La-based scale up are shown (see Chapter 7.3). Finally, conclusions, as well as a brief outlook, are summarized in Chapter 8.

2. The fermentation process

2.1. A Definition of fermentation process and cell culture

"Fermentation c'est la vie sans l'air"

"Fermentation is life without air" (Pasteur 1822-1895)

The biological conversion under the absence from oxygen is historically the term for fermentation [4]. Nowadays fermentation is defined as

"*The chemical breakdown of a substance by bacteria, yeasts, or other microorganisms, typically involving effervescence and the giving off of heat*." [5]

The term cell culture describes the growth of a certain cell population to a larger population under defined conditions [6].

Technically these two terms describe two totally different function of a cell. A good example can be given with Saccharomyces cerevisiae (i.e., baker's yeast): Under anaerobic conditions it produces alcohol, a classical fermentation. The same cells produce other yeast cells when the grow conditions are aerobic [7]. This simple example shows, how one system parameter can change the whole metabolism of a cell.

2.2. From History to Future

Over 5,000 years ago mankind started to use fermentation without any awareness of microorganisms and the principals of biotechnology. From the first products that were produced in an industrial scale by a biotechnological process in the middle of the 19th century (e.g. manufacturing of lactic acid by Böhringer) it took until the 20th century to reach the pharmaceutical industry [8].

Ever since the industrial use of cells and microorganisms, their performance regarding their mechanical and chemical resistance, as well as their growth rate and production performance were improved: from time and cost intensive random mutagenesis and screening techniques in the past, to recent research and development trends that aim on exact metabolic engineering of cells [9]. An improvement of microorganisms has to go hand in hand with an improvement of the production process. Key component of this production optimization is the bioreactor. An optimal dimensioning and design is essential for its performance.

Since the biopharmaceutical industry is a rather conservative industry (see all the regulations that need to be satisfied, e.g. FDA, GMP), a validated process is rarely replaced with a new innovative process. Often, this is motivated by a lack of process understanding. Consequently, further research will be necessary to get the industry away from the black-

box model of a bioreactor to an integrated understanding of the impacts of process parameters and controls to cell culture or fermentation process [10] [11].

2.3. Oxygen supply as key to an optimal production

Within the pharmaceutical industry the use of recombinant DNA has led to a trend in biopharmaceutical proteins. Garcia et al. [12] provides a comprehensive review on the evolution of this branch and its future.

It is shown, that most of recombinant protein-based products are either expressed by the bacterial E. coli or the mammalian CHO cell. These two microorganisms form the backbone of this industry where different production characteristics have to be taken into account.

E.coli, is a bacterium with rather robust mechanical properties, and can resist comparably high levels of shear stress. In an aerobic fermentation, it has a high oxygen demand, and is often oxygen limited in the exponential growth phase [3]. Besides the reduction of the grow rate - an unintentional metabolism can be the results. E. Coli produces under anaerobic conditions acetate, which reduces the growth rate and the biomass yield [13]. Figure 2-1 shows the variation on how the specific growth rate of different microorganisms react to an oxygen limitation.

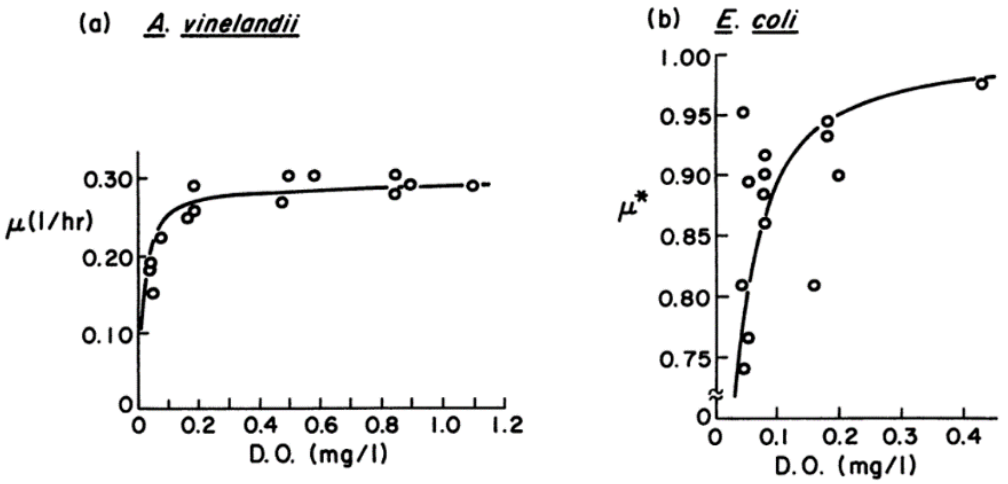

Figure 2-1 Growth-rate dependence on DO for (a) Azotobacter vinelandii, an aerobic organism, and (b) E. coli, an facultative organism, that grows anaerobically at about 70% of its aerobic growth rate.

$$\mu^* = \frac{\mu - \mu_m^{anaerobic}}{\mu_m^{aerobic} - \mu_m^{anaerobic}}$$ [7]

CHO cells on the other hand have a low oxygen demand and are rather sensitive to mechanical stress. Not only the agitation has a negative influence to the growth rate, even

the bursting of gas bubble on the liquid surface is suspected to have a cell damaging effect [14].

Since microorganisms can only metabolize oxygen that is dissolved in the cultivation media the Oxygen Transfer Rate (see Chapter 3) has a fundamental importance to the process. In an STR oxygen is usually fed at the bottom of the vessel through a sparger. The sparger, in combination with the agitator of the reactor, is supposed to ensure a good distribution of gas bubbles inside the reactor. The design of the sparger, as well as the type of impellers used have a huge influence on the capability of the system to disperse gas in the liquid phase [15]. Especially in large bioreactors an inhomogeneous oxygen distribution can be the result of a non-ideal sparger and agitator design –Figure 2-2.

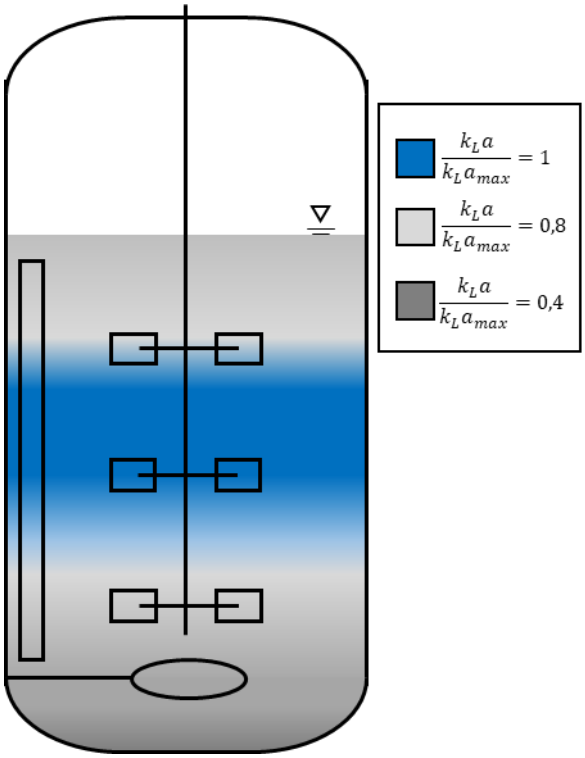

Figure 2-2 Inhomogeneous oxygen distribution in a STR © ZETA

To achieve a defined OTR is an essential task. For E. coli a maximum is attempted with a high gassing rate and agitation speed, to generate a high growth rate. For CHO cells the challenge is delivering a sufficient oxygen supply by keeping the stress to the cells at a minimum [1].

In summary it can be said, that the OTR is of importance for any aerobic process and is explained in detail in Chapter 3.

3. Oxygen transfer rate

In a gassed fermentation process, the oxygen transfer rate describes how fast oxygen is dissolved from gas bubbles into the liquid phase, e.g., the cultivation media. This rate is described by the formula:

$$OTR = k_L a \ (C^* - C) \quad (1)$$

Where $k_L a$ is the volumetric oxygen mass transfer coefficient, C the oxygen concentration in the liquid, and C^* the saturation concentration of the oxygen in the liquid. The $k_L a$ is a combination of two coefficients:

- The mas transfer coefficient k_L that combines all the different resistance to mass transport from the gas to the liquid phase, i.e., $^1/_{k_L} = \sum {}^1/_{k_i}$
- a is the gas-liquid exchange area per unit liquid volume.

Since the k_L and the a value are hard to measure separately, they are often combined to one parameter [16].

This combination makes the $k_L a$ value strong dependent from the process conditions as shown in Figure 3-1.

A good example for the influence of the properties of the cultivation media to the $k_L a$ value is the feeding of anti-foam. In a bacterial fermentation processes high gassing rates and agitator speeds are needed to ensure a high $k_L a$-value. Foam formation is the consequence and has to be prevent. So antifoam (often silicon oil) is added to the fermentation. This oil is a second liquid phase and forms a layer between gas bubbles and the liquid phase. This has a huge influence on the *kl* value, but the oil also effects the bubble size and so the interface area a [17].

Morao et al. [17] showed that an antifoam addition in an low concentration significantly lowers the $k_L a$. However at an certain concentration, the $k_L a$ increases again by adding more antifoam.

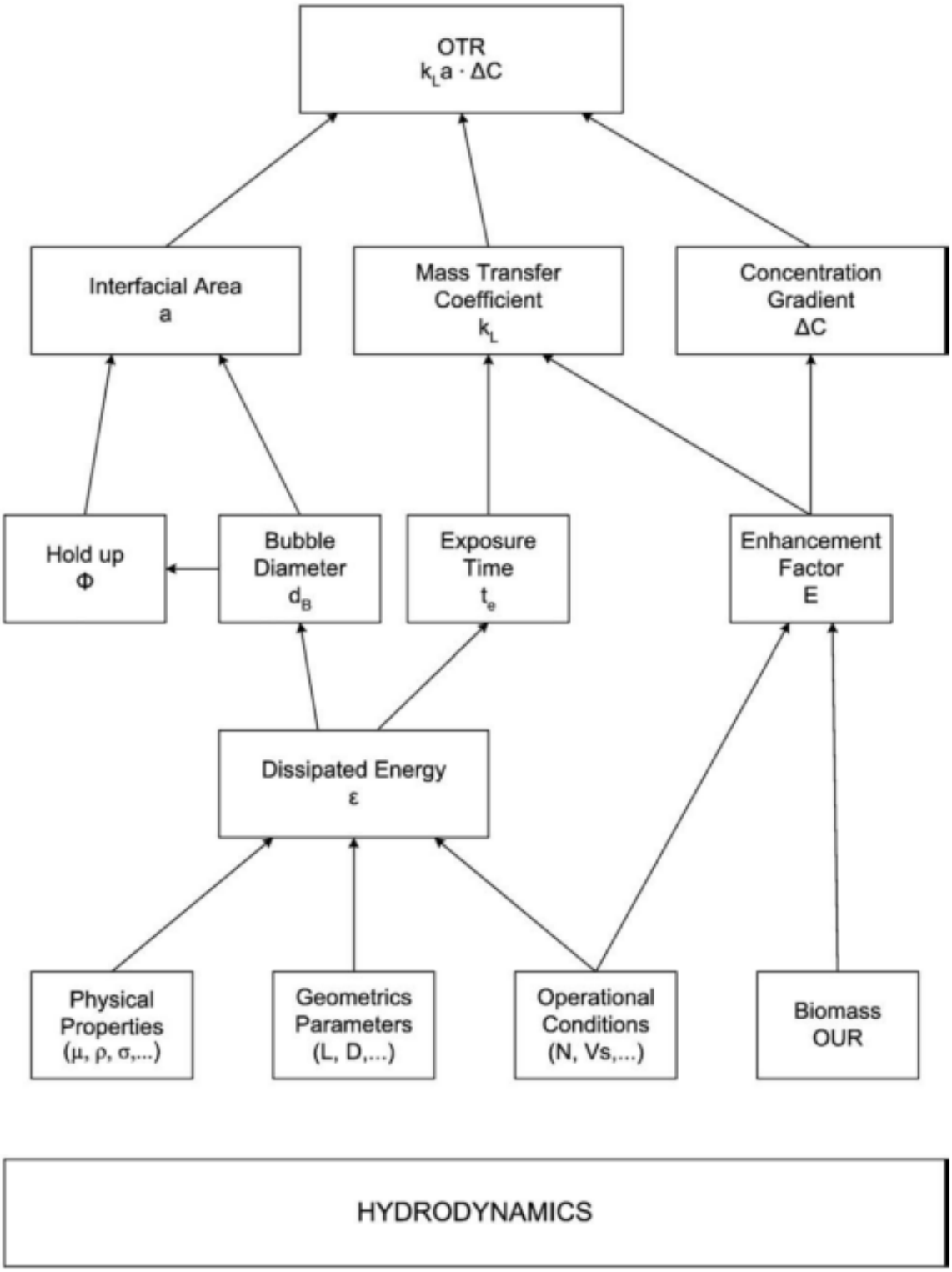

Figure 3-1 Correlation between OTR, the $k_L a$ coefficient and hydrodynamic parameters in STR [16]

3.1. Prediction of the k_La

Because of the improvements in the metabolic engineering of cells, the requirements from the customer to their plant (e.g. bioreactors) have changed within the last years. With these high performance microorganisms, coming out of a laboratory scale, it needs to be ensured, that the production scale has similar process parameters.

Predicting the k_La value, and hence ensuring a certain OTR in a bioreactor, is a major challenge. Furthermore, in more and more User Requirement Specifications (URS), customers request a certain k_La value for the bioreactor to be provided by a supplier.

There is a wide range of correlation equations to calculate a k_La value, most of them are based on the isotropic turbulence theory from 1944 [18].

$$k_La = C_1 \left(P_g/V_L\right)^{C_2} \vartheta_s^{C_3} \tag{2}$$

Where C1, C2 and C3 are coefficients depending on the system.

Gomez et al. lists 20 combinations of different coefficients for stirred tank reactors and over 10 different for dimensionless correlations of the k_La value like the formula of Nishikawa et al [16].

So choosing the right formula to calculate the k_La value for a fermenter is rather gambling than science.

Most of the system parameters, like the properties of the cultivation media, the fermentation temperature and the operating conditions depend on the preferences of the microorganism and are often predefined in a laboratory scale. These parameters are then scaled up and define the main parameters of the production scale [19]. These scale up procedures variate from simple rule of thumbs concepts to fundamental methods and dimensional analyses.

This was the reason for the financing industrial partner ZETA to focus on the measurement of k_La values. The present thesis hence focuses on establishing technology to be able to gather real data from the plants ZEAT is building.

4. Measuring methods of the k_La-value

The dependency of the k_La value to a large number of process parameters challenges also its measurement: the conditions during the k_La characterization procedure have to be as similar as possible to the final process.

Furthermore, for a measurement at an industrial plant other requirements have to be taken into account: no chemicals and their formulations other than for the process validated can be used. Also, mechanical changes on the equipment are often impossible, and often the process control for the test runs has to be done manually.

The measurements have to be done during a downtime, since the measuring method cannot be used during production.

4.1. Methods

There are many different methods, that can be classified in chemical, biological and physical methods. During a fermentations process the oxygen supplied is consumed by the microorganisms so that a concentration change of oxygen in the broth can be described by:

$$\frac{dC}{dt} = OTR - OUR \tag{3}$$

Here the Oxygen Update Rate is described by the metabolism of the microorganism [16].

Since the tests are done during an absence of biology and any chemical oxygen consumption the OUR can be set zero so that the concentration change is only a function of the OTR.

$$\frac{dC}{dt} = k_L a \ \left(C^* - C\right) \tag{4}$$

In oxygen saturated water $(C^* - C)$ equals zero, so to measure the k_La, C^* or C have to be changed to measure the balancing process. Two standard methods, that meet all the limitations were tested and compared.

Dynamic Step Method (DSM)

Here the oxygen concentration of water is set to zero by degassing it with nitrogen. Once the nitrogen stripped all the dissolved oxygen, the system is gassed with pressurized air again. With the initial conditions that $C_{(t=t_0)} = C_0$ the concertation change can be integrated to

$$ln\left(\frac{C^* - C_l}{C^* - C_0}\right) = -k_L a\ (t - t_0) \tag{5}$$

and describes the time course of the concentration after starting the aeration [16].

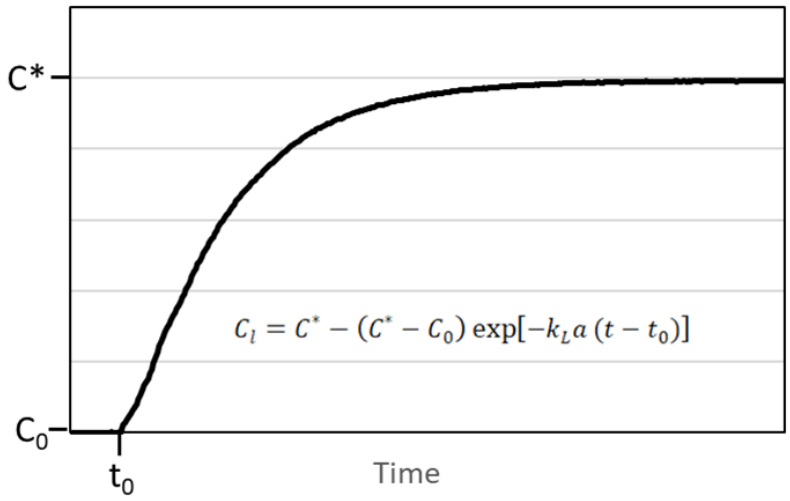

Figure 4-1 Schematic illustration of the concentration change of a system, reacting to a step change of the saturation concentration

Nitrogen gas is a commonly used media in fermentation processes, so often it is available at an industrial plant. However, tests involving lager bioreactors (e.g. 15000L) have shown (test results and details are confidential and available to ZETA GmbH), that a fast switch from nitrogen to air in the gassing system is a challenge for the manual process control. For high gassing rates the air system can also show quite a delay to reach the full volumetric flow rate, which can also be a problem for measuring a system with very high k_La-values.

Dynamic Pressure Method (DPM)

With the DPM no other media than pressurized air and water (or the fermentation broth) are needed. The concentration change of the system is done by changing the working pressure of the reactor and so the saturation concentration of oxygen in water [16].

According to Henry's law the solubility of air in water can be described as

$$H^{cp} = \frac{C^*}{p} \tag{6}$$

So that the concentration change due to a pressure change is approximately

$$\frac{C_2^*}{C_1^*} \approx \frac{p_2}{p_1} \tag{7}$$

It has to be noted, that the assumption of air as a single component is a major simplification. Scargiali et al. [20] shows correlations to correct the measured k_La by taking the solubility

of oxygen and nitrogen into account. Also the sudden pressure change and so the change of the bubble sizes has a negative influence on the accuracy for this measuring method.

Blažej et al. [21] shows that k_La-values from the DPM are up to 100% higher than the k_La-values measured with the DSM.

Although the k_La-values of the two methods are hardly comparable and the fact that the DSM is more often used in publications, the DPM has some benefits and still can be used to investigate spatial inhomogeneities of the k_La values (e.g., the effect of the impeller position inside an STR).

4.2. Oxygen sensors

The calculated time for a concentration change from 0 to 90% for a k_La-value of 1000 h^{-1} during the DSM is 8.3 seconds. Thus, a fast response time of the oxygen probe is essential for a good measurement.

There are two types of oxygen probes that are mainly used for bioreactors, (i) the Clark electrode, which is getting more and more replaced by (ii) optical sensors.

The measurement of the Clark electrode is based on an oxygen reduction, taking place behind an oxygen permeable membrane. Optical sensors are based on quenching of luminescence, so the probe reacts to the luminescence intensities in the absence and presence of oxygen [22].

The main advantage of the optical sensor is, that there is no reduction reaction, that consumes time and oxygen. This reaction results in a longer response time and has a negative influence on the measurement [23].

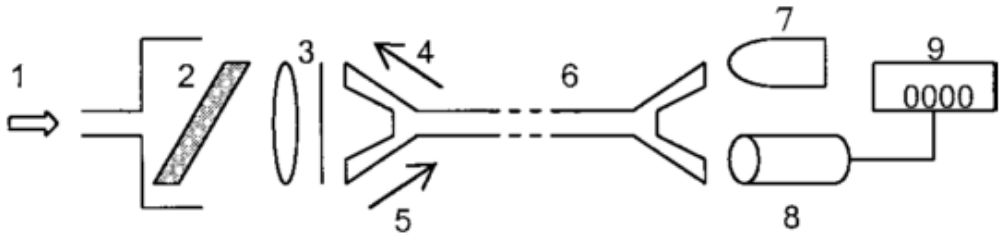

Figure 4-2 Schematics of an optical sensor. (1) gas or liquid path, (2) lumophore dispersed on oxygen permeable membrane, (3) lens and filter, (4) exciting radiation, (5) fluoresccent radiation, (6) optical fiber, (7) LED/Laser, (8) photodiode, and (9) display [24]

Figure 4-2 shows the assembly of an optical oxygen sensor. Another advantage of the sensor is, that the membrane with the lens is connected via an optical fiber to the rest of the sensor. With an optical fiber cable, a very small design of the sensor head is possible. Two oxygen

sensors of the same manufacturer are used in the present thesis. They have the same measuring principle and only deviate in their design. The OXYPro WR-120 (Figure 4-3 a) sensor is used through a standard nozzle (e.g., Ingold nozzle) and has the advantage of a compact a robust design. The FTM2-HP (Figure 4-3 c) sensor uses an optical fiber cable to get a much smaller sensor head. Because of the small construction it is perfect to be mounted in a flow through cell.

a) © PreSens

b)

c)

d) ©ZETA

Figure 4-3 Used oxygen sensors a) OXYPro WR-120 b) mounted in an Ingold Nozzle c) FTM2-HP-1/4"-PSt3-OIW d) mounted in a flow through cell

4.2.1. Response time

The optical oxygen sensor has an oxygen permeable membrane Figure 4-2 (2) so that the sensor reacts to an concentration change according to a first order reaction [25].

$$\frac{dC_{me}}{dt} = \frac{(C_L - C_{me})}{\tau_r} \tag{8}$$

Here τ_r is the reaction time of the sensor that is defined as the required time for measuring a concentration change of 63% in case a concentration step change is applied to the sensor. This value has to be taken into account when calculating the k_La of a STR with the measurement data of an oxygen probe. With (4 that describes the concentration change of

the system, and (8 the correlations between the measured concentration change and the k_La-value of the system can be calculated.

$$C_{me} = C^* + \frac{(C^* - C_0)}{1 - \tau_r \cdot K_L a}\left[\tau_r \cdot K_L a \cdot \exp\left(\frac{-t}{\tau_r}\right) - \exp(-K_L a \cdot t)\right] \quad (9)$$

4.2.2. Influence of gas bubbles

A gassed bioreactor represents a two phase system with a continuous liquid phase and a dispersed gas phase. Oxygen can diffuse from both phases to the membrane of the sensor, with the issue, that the diffusion from gas is much faster. Since only the oxygen concentration of the liquid is of interest, it has to be assumed that the presence of gas bubbles has a negative influence on the measurement.

The measuring method with a flow through cell is able to deliver a bubble free sample stream for the sensor, the advantages are investigated in the experimental part of this thesis (Chapter 5).

5. Measuring with a flow through cell

To improve the standard measuring methods, a method with a flow through cell equipped with an oxygen sensor was developed within the present thesis (see patent number A20182/2018, Status „Pending“). This measuring method positions the sensor outside of the vessel. The actual measuring point is reached with a tubing inside of the fermenter, so that any position can be investigated, see Figure 5-1.

A full mapping of the fermenter, regarding its oxygen distribution is possible and zones, where microorganisms are undersupplied with oxygen can be determinate.

5.1. Setup

With a peristaltic pump, a constant sample stream is sucked out of the vessel and transported to the oxygen sensor, and then back into the vessel.

The internal and external tube are connected through a standard nozzle, in our chase an Ingold nozzle. Here it is important, that the outlet and the inlet are not causing a short circuit. Additionally, the tip of the inner tubing is equipped with a membrane, to strip any gas bubbles from the probe stream, so that the oxygen sensor is not influenced by a two phase mixture.

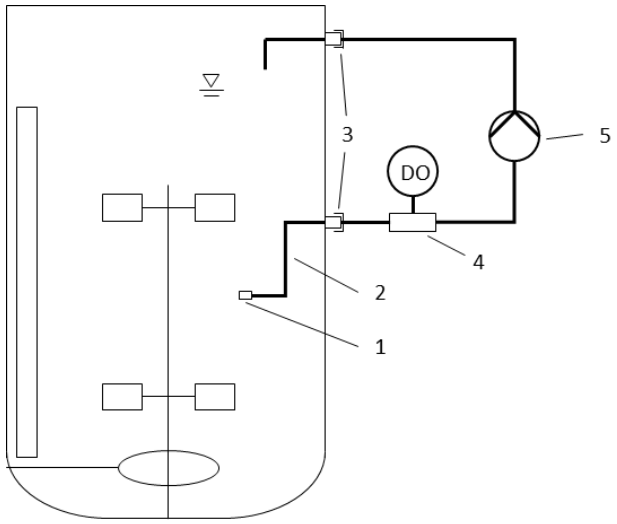

Figure 5-1 Schematic illustration of the measuring method. (1) membrane (2) pipeline (3) Connector to the reactor (4) flow through cell (5) peristaltic pump

5.2. Influence on the measured value

It is obvious that the measuring method must not have an influence to the measuring results. For this, two problems have to be taken into account. An ideal plug flow has to be ensured in the pipeline, to avoid any back mixing of the probe stream. This results in a small pipe

diameter and a high flow rate (i.e., high Reynolds number). On the other hand, the pressure drop from the measuring point to the sensor has to be at a minimum, so that the sampled liquid does not degas on the way to the sensor.

For a full turbulent regime, a Reynolds Number of 8,000 has to be ensured. Thus, for a ¼'' tubing with an inner diameter of 4.57 mm, the volumetric flow rate has to be 1.7 l/min.

$$Re = \frac{\vartheta \, D_i}{v} \tag{10}$$

The pressure loss caused by the pipe friction can be calculated for this flow regime with

$$\Delta p = \zeta \, \frac{l}{D_i} \, \frac{\rho u_i^2}{2} \tag{11}$$

ζ for Re=3,000 to Re=10^5

$$\zeta = \frac{0.3164}{\sqrt[4]{Re}} \tag{12}$$

So the pressure loss for the tubing used results in $\Delta p \approx 0.1 \left[{}^{bar}/_{m} \right]$ [26].

If this pressure loss has a negative influence to the measurement will be investigated in Chapter 6.3.

5.3. Further applications for the Flow Through cell

The possibility of generating a bubble free probe stream out of a gassed bio reactor can be used for various different applications.

For example, a conductivity probe, mounted in the flow through cell can be used for mixing time studies in gassed systems. At the moment, the method is not used for the actual fermentation process during a production, because it does not meet the GMP requirement in terms of clean ability and process safety. A further development in the future could lead to new ways of process controlling.

6. Application of the k_La measuring methods

6.1. Experimental setup

For the tests a 20L and a 150L stirred tank reactor are used. The reactors are equipped with a central agitator, a ring sparger for gas supply and four baffles.

The properties of the vessels are listed in Table 6-1

		20L Fermenter	150L Vessel
Working volume	V	20L	150L
Diameter	D	0.265m	0.530m
Baffle width	B	0.1 D	
Filling height	H	1.36 D	
Agitator diameter	D_A	D / 3	
Sparger Diameter	D_S	0.7 D_A	
Agitator 1	H_{A1}	1.3 D_A	
Agitator 1	H_{A2}	1.9 D_A	
Sparger height	H_S	0.6 D_A	

Table 6-1 Reactor design - properties

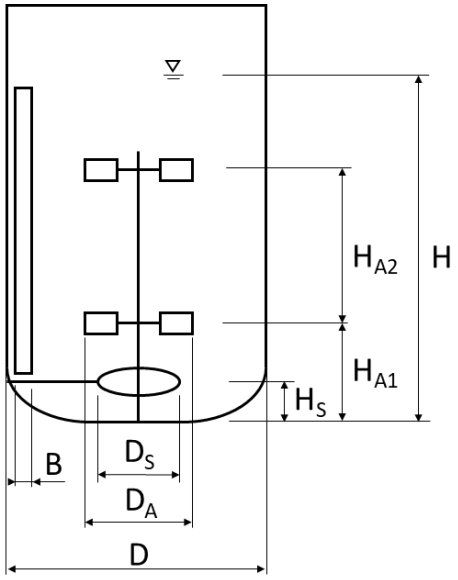

Figure 6-1 Reactor design

The vessels are connected to a gassing system, where the gassing rate is measured and controlled and a fast switch between nitrogen and air is possible for the DSM experiments. Unlike the glass vessel, the 20L fermenter is designed for a working pressure of up to 4 bar(g) for carrying out the comparison tests between the DSM and the DPM.

The central agitator is equipped with two Rushton stirrers mounted on the shaft.

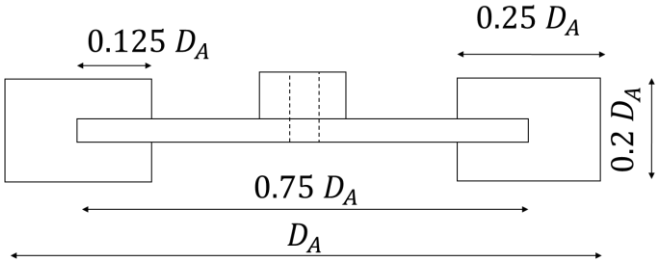

Figure 6-2 Properties of a Rushton agitator

6.2. Measuring the response time of the sensor

Since the diffusion of the oxygen to the sensor membrane causes a delay according to (8), the response time of the sensor has to be determined. For this, a fast concentration change from degassed to oxygen saturated water is generated and the response of the probe is measured.

It is important that the response time of the sensor is measured under similar conditions as the tests are carried out (e.g., similar pressure and temperature).

Since the influence of gas bubbles to the sensor are investigated as well, the response time is also measured for a gas phase with a change from nitrogen to air.

For the tests in water two beakers, one saturated with oxygen and one degassed with sodium sulfite were prepared, and the sensor was calibrated. The sensor was then put from one breaker to the other logging with its maximum sampling rate of 5 s^{-1}.

The tests with gas were carried out in a flow though cell. The cell was connected to a three-way valve for a fast switch between nitrogen and air. It is important, that no backpressure occurs in the cell so that the tests are done at atmospheric conditions.

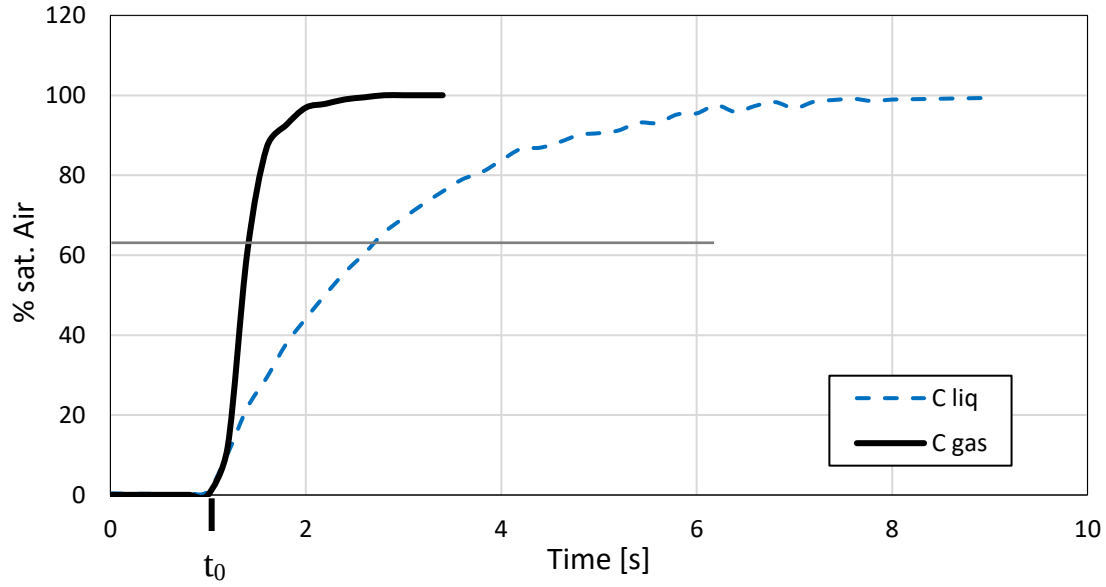

Figure 6-3 Measured concentration change of an oxygen sensor after an oxygen step change

Figure 6-3 shows the results of the measurements in the gas and liquid phase. The measured response time for a concentration change in water was 1.85 [s]. The response time of the sensor in a gas phase is - with 0.25 [s] - significantly faster.

6.3. Validation of the flow through cell

To compare the flow through cell with the standard sensor, and to proof that the method does not have a negative influence on the measuring results, the system was set up in the 20L

fermenter. The standard probe was mounted at the bottom through an Ingold nozzle and the tube of the flow through cell, with a length of 0.5m, was lead to the same measuring point below the sparger.

The gassing rate and agitator speed were set to the lower end of the investigated parameter range (i.e., 140 rpm; 0.5 vvm) so that no bubbles, rising from the sparger are pushed back down to the sensors. The pump of the flow through cell was set to 1.7 L/min and the DSM was carried out.

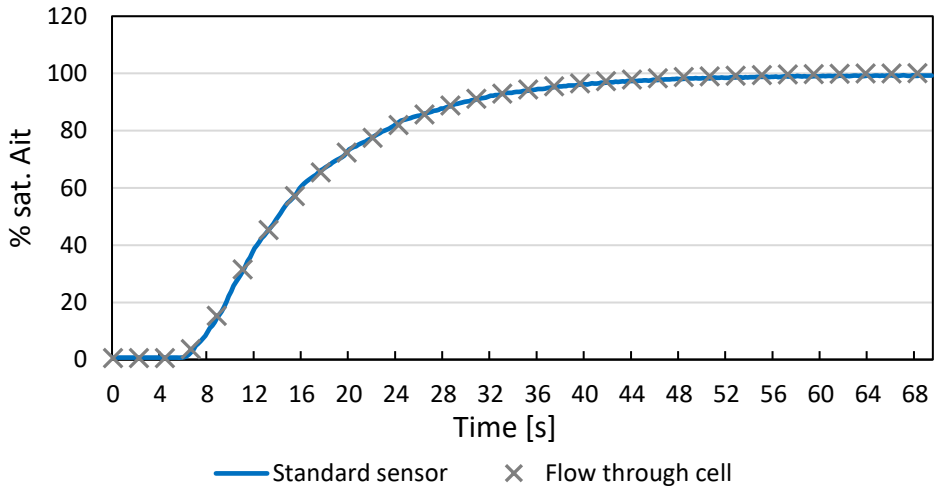

Figure 6-4 Concentration measurement of a standard oxygen sensor and a flow through cell

Figure 6-4 shows the concentration curves of both measurements. The calculated k_La-values are 340.6 [1/h] for the standard probe and 344.3 [1/h] for the flow through cell. So the pressure drop of the pipe does not influence the measurement.

6.4. Influence of gas bubbles

To investigate the influence of the two phase system to the results of the measurements, tests with different gassing rates, agitator speeds measuring positions were done with both systems, i.e., the standard probe and the flow through cell.

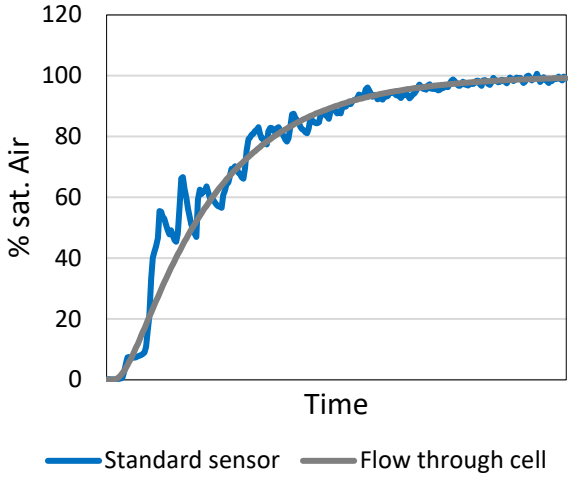

Figure 6-5 Noisy signal caused by large gas bubbles

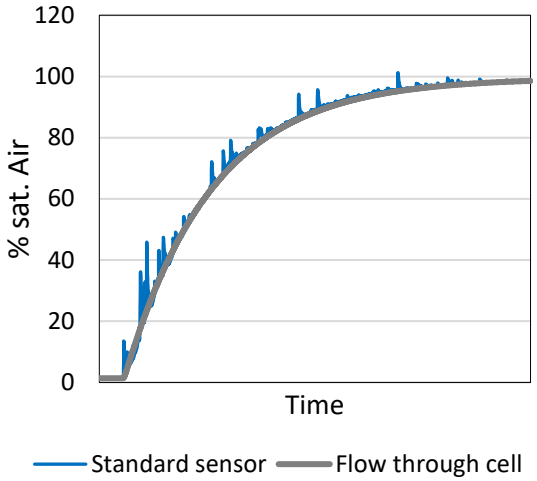

Figure 6-6 Noisy signal caused by small gas bubbles adhering onto the sensor head

The tests showed, that when the dispersion of the gas phase is high enough the standard probe is not negatively influenced. Figure 6-5 shows, that at higher gassing rates the bigger air bubbles add a certain noise to the signal. On the other range of the setup, when the measurements are carried out at a low agitator speed and gassing rate, bubbles start to adhere to the sensor and influence the signal (Figure 6-6).

6.5. Comparison of DSM and DPM

Since both measuring methods have their advantages and drawbacks regarding to their usability at an industrial site both methods are carried out with the new flow through cell and their results are compared. The measurements are done in the 20L fermenter. For the experiments the measuring position is at sparger height at mid between the agitator shaft and the vessel wall. The agitator speed is set to 700 rpm and the gassing rate to 2.0 vvm.

6.5.1. Dynamic Step Method (DSM)

For the DSM the fermenter is filled with deionized water. The water is then degassed with nitrogen until the oxygen concentration is constant below a value of 0.1% Air. Then the gassing is rapidly changed back to air at the set gassing rate. Figure 6-7 shows the setup for the 20L fermenter.

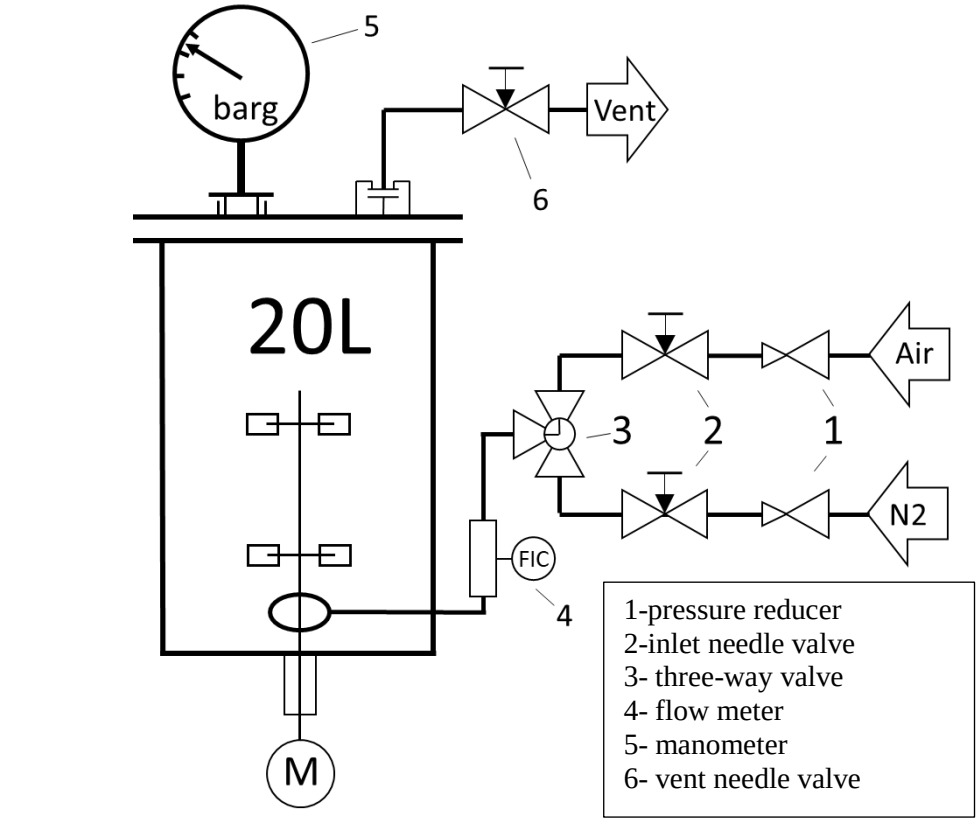

Figure 6-7 Setup of the 20L reactor for the DSM

The concentration change, from 0-100% saturated air is then logged at a measuring rate of 0.2 s. Since the pressure of the system has an influence on the k_La value, the tests are done from 0 bar(g) to 1bar(g) at 0.2bar steps to compare them to the DPM. The system pressure is adjusted with a needle valve in the vent line at the vessel lid.

Each test is done five times to see how reproducible the results are.

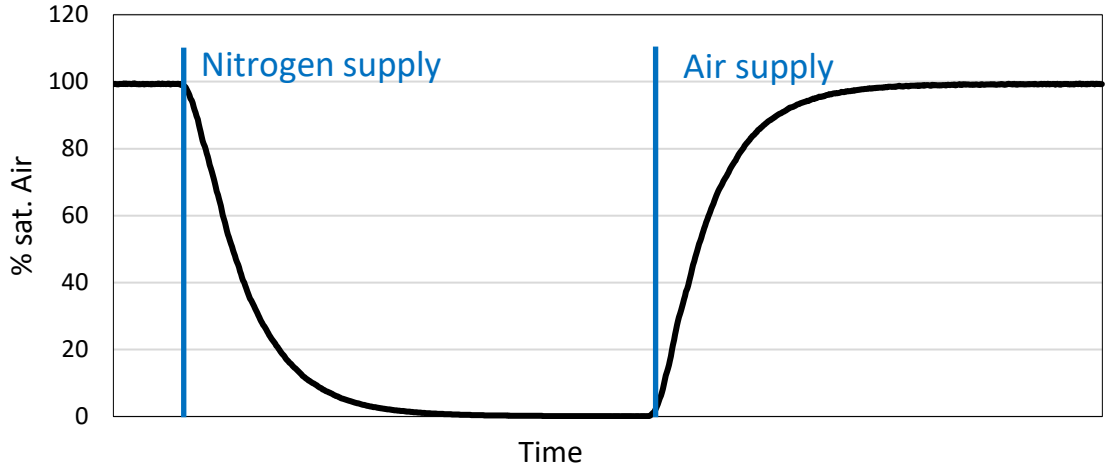

Figure 6-8 Schematic illustration of the concentration change when using the DSM

6.5.2. Dynamic Pressure Method (DPM)

For the DPM a quick pressure change between 0.2 and 1.0 bar(g) has to be ensured. A simple closing of the vent pipe and using the backpressure of the gassing rate is by far not fast enough. Therefore, a second inlet of compressed air is mounted in the headspace of the vessel.

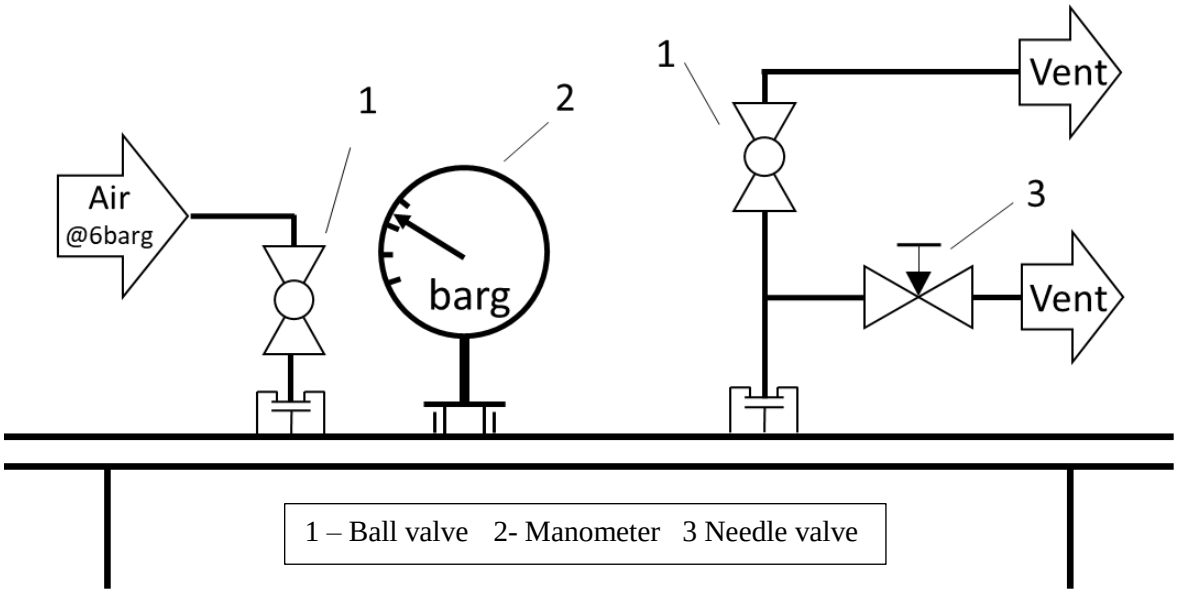

Figure 6-9 Setup of the reactor lid for the DPM

For the tests a certain pressure, for example 0.6 bar(g) is adjusted with the flow resistance of the needle valve at a closed ball-valve. The pressure is then released by opening the ball-valve again. When the sensor is measuring the constant saturation concentration at atmospheric pressure again (e.g. C_0=100%) the test is started by closing the ball-valve and at the same time opening the ball-valve of the head pressure @6 bar(g). The valve is closed again when the head pressure reaches the target value.

With a little practice this pressure change can be done in under 2 seconds by hand.

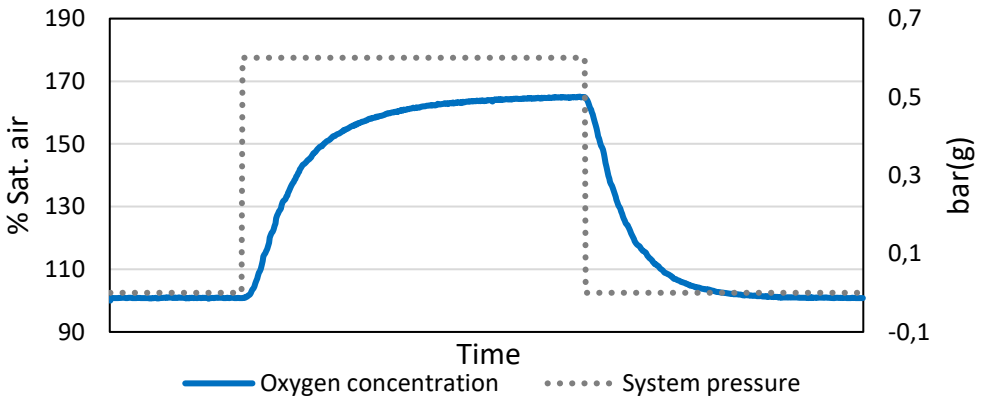

Figure 6-10 Schematic concentration change during a DPM

6.5.3. Results

As already explained the k_La-values of the two methods are not comparable, Figure 6-11 shows the results of the DSM and DPM for different head pressures. The k_La values of the DPM are up to 45% higher than the once measured with the DSM. This finding correlates with the conclusion of Blažej et al. [21].

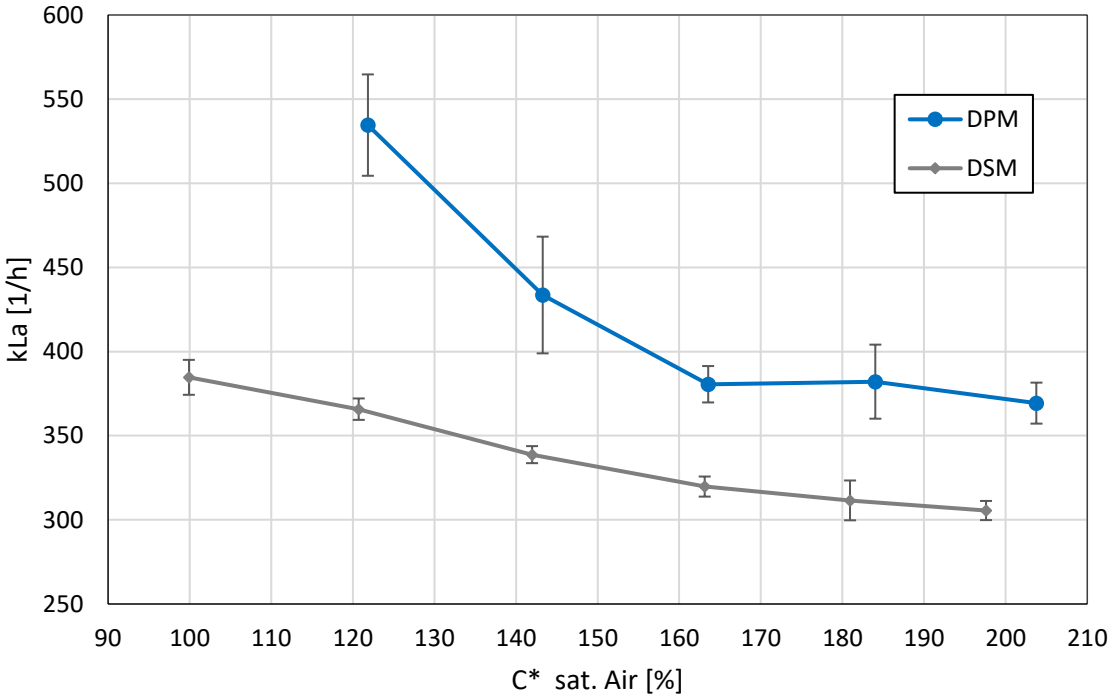

Figure 6-11 Comparison of the DSM and DPM with the standard deviation of five measurements

Since the DSM is easier to handle, the corresponding results are clearly more reproducible. The standard deviation of the DPM is a result of the manual handling of two valves, this could be optimized by an automated system.

7. Measuring a 20L and a 150L reactor

7.1. Classical measurement via liquid-phase concentration change

To show the usage of the developed measuring system, k_La-measurements at the 20L and 150L vessel are done at three different positions with 25 different operating points. It has to be mentioned, that since the developed method measures the oxygen concentration change at a fixed point, the resulting value cannot be strictly defined as k_La value. This is due to the fact, that the measured concentration change is a result of the oxygen getting dissolved by the local k_La-value and convection and diffusion which transports oxygen from other areas to the measurement location. In case these other areas have a very different (e.g., higher) oxygen dissolved concentration, the estimated k_La value would be different (i.e., too high). Consequently, a k_La-like coefficient termed as the local oxygen supply rate "k_La*" is used to indicate the local rate of oxygen supply (Figure 7-1).

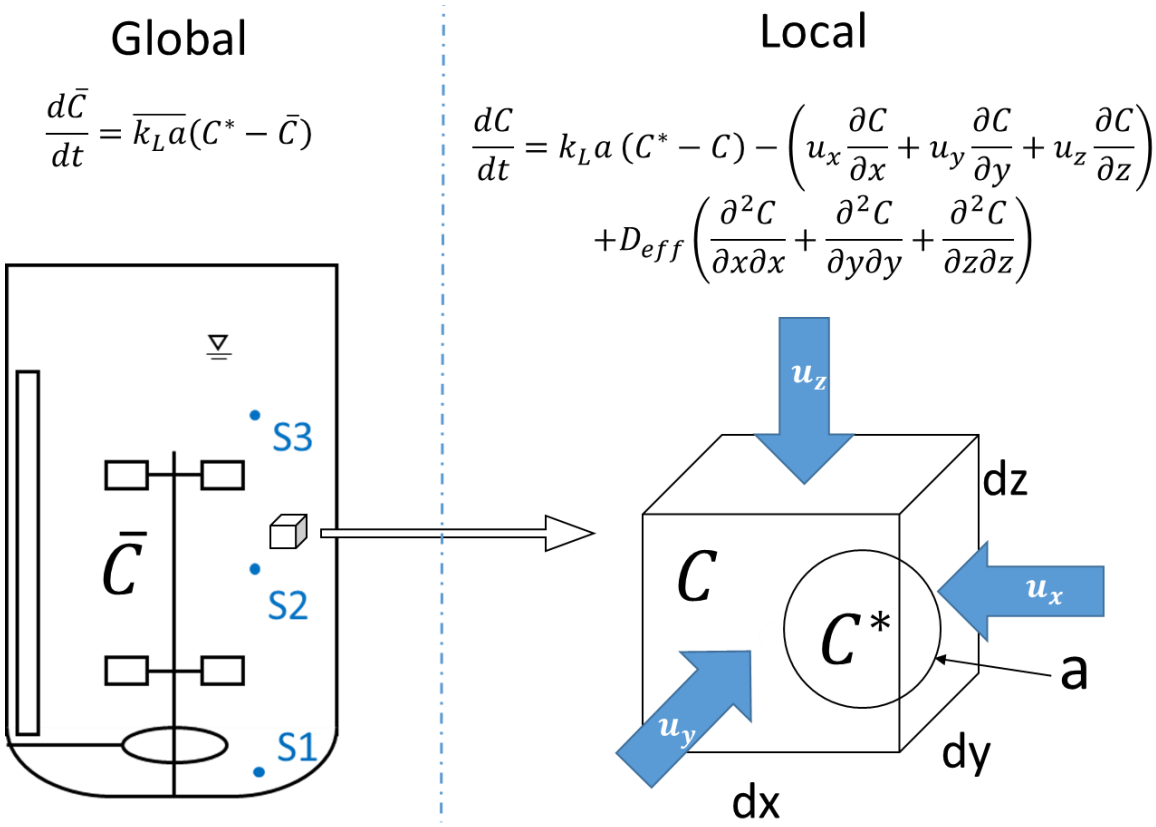

Figure 7-1 Concentration change for a global and a local k_La measurement

Since all the oxygen is supplied by diffusion, described by (4 the measured k_La* value fluctuates around the global k_La value.

$$\overline{k_L a} = \lim_{i \to \infty} \frac{\sum_0^i k_L a_i^*}{i} \quad (13)$$

The measurements in the reactor were done at (i) S1: below the sparger (ii) S2: between the stirrers and (iii) S3: below the surface of the water.

The results of the 20L vessel already show an inhomogeneity between the different measuring points. Figure 7-2 a and b show that this inhomogeneity occurs at high agitator speeds and at high gassing rates. For 700 rpm and a gassing rate of 2.5 vvm the $k_L a^*$ at the top of the reactor is more than 25% higher than the $k_L a^*$ at the bottom. The measurements of the 150L reactor show similar results (Figure 7-2 c and d).

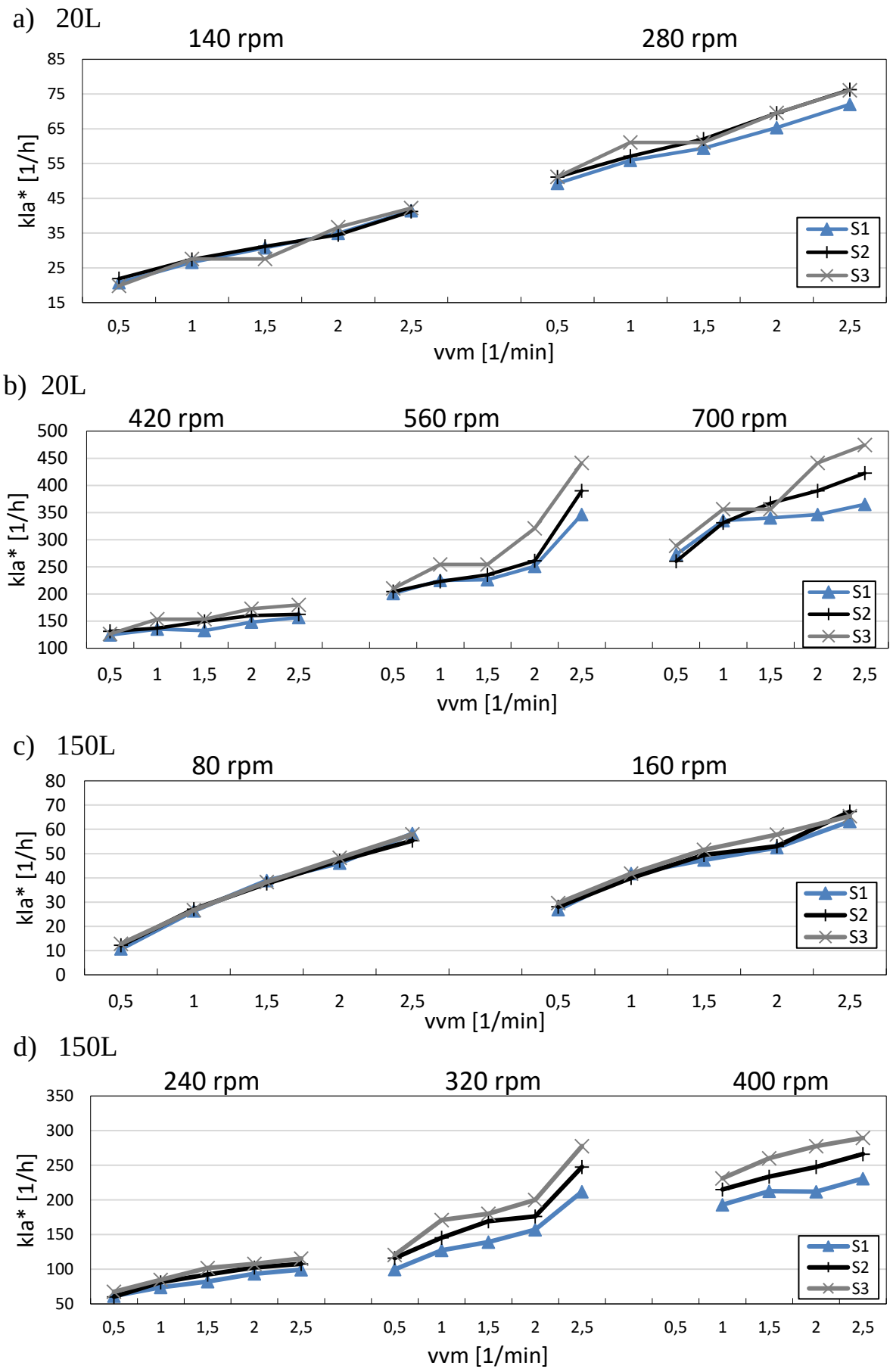

Figure 7-2 Results of the k_La^* measurements in the 20L and 150L reactor

7.2. Measurement via exhaust air concentration change

To compare these measurements with a global k_La value, the attempt of measuring it over a simple mass balance between the inlet and outlet of the gas stream of the reactor during a DSM was made. The test was done in the 20L vessel at a gassing rate of 2.5 vvm and an agitation speed of 700 rpm. The oxygen concentration was measured with the OXYPro WR-120 in the headspace (5L) of the reactor.

The concentration change of the gas stream was calculated with (5. Since the head space of the reactor is filled with pure nitrogen at the beginning of the experiment the concentration change of the exhaust air is calculated by assuming an ideal mixing within the head space and the gas stream leaving the liquid phase of the reactor. The so calculated concentration change is the compared to the measured.

Figure 7-3 shows the calculated concentration change of the exhaust air for an k_La of 1 [1/h] and 1,000 [1/h], as well as the measured concentration change. As shown it is not possible to predict the global k_La by measuring the exhaust air. The concentration change in the bubbles leaving the liquid is too small to have a significant impact on the concentration change of the head space volume.

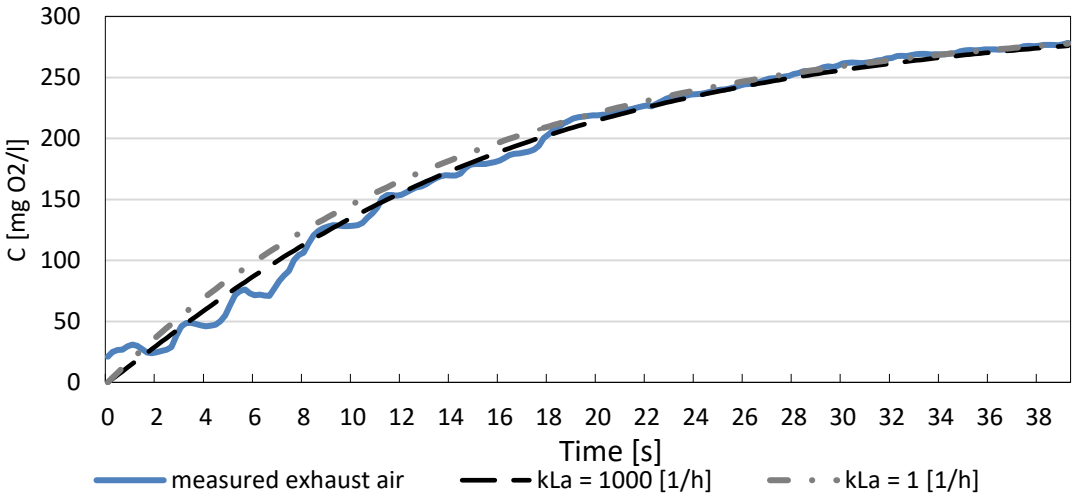

Figure 7-3 Measured and calculated concentration change of the exhaust air for different kLa values

7.3. Scale up

Since the two measured systems only differ regarding their volume, a comparison of their k_La values is done to check how scalable the simple turbulence theory according to (2 is. Instead of the agitator speed and the gassing rate the power input per vessel volume and the superficial air velocity are used. With the power numbers of the agitators the power input can be calculated for each agitator speed and gassing rate.

Table 7-1 shows the power input for each operating point. The power numbers were measured in the 150L vessel and are valid for the whole agitator, so two Rushton stirrers on one shaft. Also, the power distribution of the agitator bearings has been considered.

	Gassing	0.5 vvm [min^{-1}]	1 vvm [min^{-1}]	1.5 vvm [min^{-1}]	2 vvm [min^{-1}]	2.5 vvm [min^{-1}]
	Power Nr.:	6.35	4.84	4.33	4.12	3.94
	RPM	**P/V [10^{-3} W/m³]**				
20L	**140**	0.022	0.017	0.015	0.014	0.013
	280	0.174	0.132	0.118	0.113	0.108
	420	0.586	0.446	0.399	0.380	0.363
	560	1.388	1.058	0.947	0.901	0.861
	700	2.711	2.067	1.849	1.759	1.682
150L	**80**	0.017	0.013	0.012	0.011	0.011
	160	0.138	0.105	0.094	0.090	0.086
	240	0.466	0.355	0.318	0.303	0.289
	320	1.105	0.842	0.754	0.717	0.686
	400	2.159	1.645	1.472	1.401	1.339

Table 7-1 Power number and power input for different operating points

Table 7-2 presents the superficial air velocity (i.e., air volumetric flow rate divided by cross sectional area) for the two vessels.

Gassing	0.5 vvm [min^{-1}]	1 vvm [min^{-1}]	1.5 vvm [min^{-1}]	2 vvm [min^{-1}]	2.5 vvm [min^{-1}]
v_s $[m/s]$ **20L**	0.00302	0.00604	0.00906	0.01208	0.0151
v_s $[m/s]$ **150L**	0.00585	0.0117	0.01756	0.02342	0.0292

Table 7-2 Superficial air velocity for different gassing rates

Since the turbulence theory relates to the global k_La, the k_La*-values of the three different measuring points were averaged (an alternative averaging of the concentrations, and then calculating the global k_La value was postponed to future work).

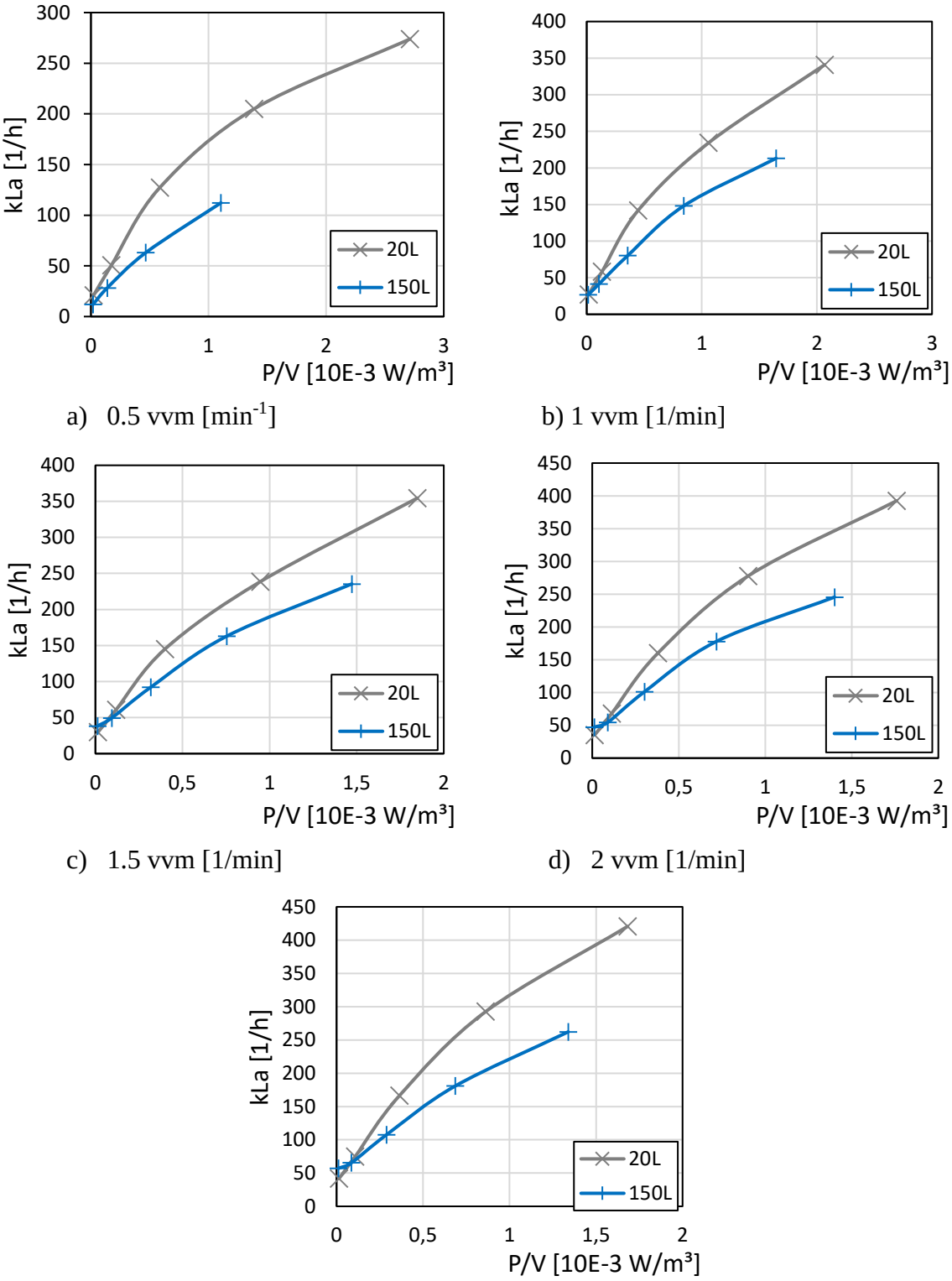

a) 0.5 vvm [min^{-1}]

b) 1 vvm [1/min]

c) 1.5 vvm [1/min]

d) 2 vvm [1/min]

e) 2.5 vvm [1/min]

Figure 7-4 Comparison of the kLa values of the 20L and 150L reactor for different gassing rates

For the two vessels the coefficients of (2 were fitted, resulting in the two following correlations:

$$k_L a_{20L} = 17 \left(\frac{P_g}{V_L}\right)^{0.52} v_s^{0.41} \quad \left[\frac{1}{s}\right] \tag{14}$$

$$k_L a_{150L} = 9.8 \left(\frac{P_g}{V_L}\right)^{0.4} v_s^{0.62} \quad \left[\frac{1}{s}\right] \tag{15}$$

$$\frac{P_g}{V_L}\left[\frac{W}{m^3}\right] ; \; v_s\left[\frac{m}{s}\right]$$

The model for each vessel fits the measuring points very well, and is ideal to predict the $k_L a$ value for different operating points.

Unfortunately, the equations are not scalable (based on identical vvm), so it is not possible to make an assumption for the 150L system with the 20L model, although all geometric properties are the same. Thus, for the practical application the challenge is finding the right model for a considered reactor design. For example, one could replace the gassing rate with some other quantity, e.g., the flow number $Fl = \dot{V}_g/(d^3 n)$ to find a better correlation in a future study.

8. Conclusion

The presented oxygen measuring method improves the standard oxygen sensors used in a stirred tank reactor regarding the flexibility of the measurement position and accuracy when measuring in a two-phase system.

The presented k_La measuring methods are capable to deliver a local oxygen supply rate and the general performance of a bioreactor can be investigated.

With these tools it is possible to analyze operating conditions and carry out process optimizations for new or existing bio reactors.

The two measured systems (e.g., 20L and 150L reactor) show a striking contrast of their k_La-values, although all their system parameters and specific operating points are identical. This shows, why the scale up of the k_La-value is a challenge and of major importance.

8.1. Outlook

Because of the significant similarity of the inhomogeneity of the two test reactors, another scale-up procedure is proposed. Based on the theory that the scale of the k_La value of an STR is defined by the power input per reactor volume and the gassing rate, it should be possible to define a k_La value for any reactor with a reference reactor within the same scale.

Figure 8-1 shows the proposed procedure.

For example, the k_La value for a STR X should be predicted. To do this, measurements of a reactor with a similar size and dimension, but a different agitator configuration shall be used. To investigate the influence of the deviating agitator geometry a smaller reactor with an easy to change agitator geometry (for example with 3D-printed stirrers) is characterized with the design of reactor A and B.

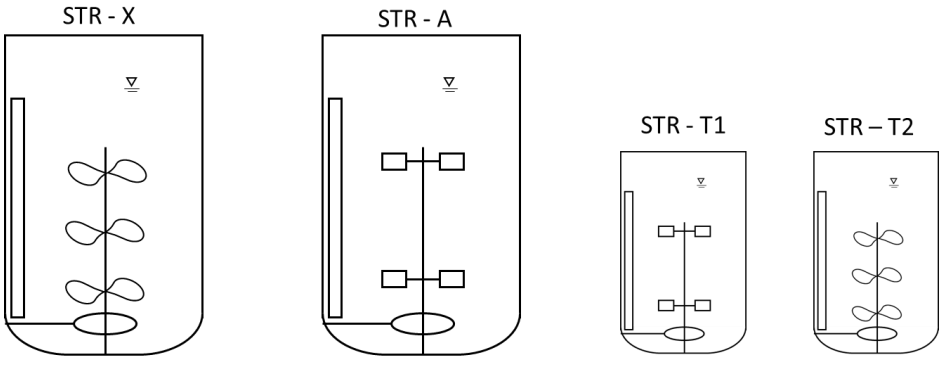

Figure 8-1 Scale up model based on the k_La ratio on different reactor designs

The new k_La is then calculated with the scale of the reactor X and the design ratio of T1 and T2.

This procedure requires an extensive pool of k_La in order to deliver a variety of STR, as well as (potentially) reliable k_La values. Further k_La studies will be necessary to proof this scale-up procedure.

9. References

[1] H.C. Vogel, C.M. Todaro, Fermentation and Biochemical Engineering Handbook: Principles, Process Design, and Equipment: Third Edition, Elsevier Inc., Waltham, 2014. doi:10.1016/C2011-0-05779-4.

[2] R. Jime, Optimization of Bacteriocin Production by Batch Fermentation of Lactobacillus plantarum LPCO10, Appl. Environ. Microbiol. 68 (2002) 4465–4471. doi:10.1128/AEM.68.9.4465.

[3] H. Chmiel, Bioprozesstechnik, 3rd ed., Springer Spektrum, Heidelberg, 2011.

[4] Fermentation, (2018). http://www.chemie.de/lexikon/Fermentation.html (accessed March 12, 2018).

[5] Definition of fermentation, (2018). https://en.oxforddictionaries.com/definition/fermentation (accessed August 20, 2018).

[6] Arshadchaudry, Cell Culture, (2004). https://www.scq.ubc.ca/cell-culture/ (accessed August 20, 2018).

[7] M.L. Shuler, F. Kargi, Bioprocess engineering: Basic concepts, 2nd ed., Prentice Hall, Upper Saddle River, 2002. doi:10.1016/0168-3659(92)90106-2.

[8] R. Ulber, K. Soyez, 5000 Jahre biotechnologie, Chemie Unserer Zeit. 38 (2004) 172–180. doi:10.1002/ciuz.200400295.

[9] Z. Dai, J. Nielsen, Advancing metabolic engineering through systems biology of industrial microorganisms, Curr. Opin. Biotechnol. 36 (2015) 8–15. doi:10.1016/j.copbio.2015.08.006.

[10] T. Heine, Modellgestützte Überwachung und Führung von Fed-Batch-Prozessen zur Antibiotikaproduktion, TU Berlin, 2004.

[11] D. Riesenberg, R. Guthke, High-cell-density cultivation of microorganisms, Appl. Microbiol. Biotechnol. 51 (1999) 422–430. doi:10.1007/s002530051412.

[12] L. Sanchez-Garcia, L. Martín, R. Mangues, N. Ferrer-Miralles, E. Vázquez, A. Villaverde, Recombinant pharmaceuticals from microbial cells: a 2015 update, Microb. Cell Fact. 15 (2016) 33. doi:10.1186/s12934-016-0437-3.

[13] S.Y. Lee, High cell-density culture of Escherichia coli, Trends Biotechnol. 14 (1996) 98–105. doi:10.1016/0167-7799(96)80930-9.

[14] Y. Chisti, Animal-cell damage in sparged bioreactors, Trends Biotechnol. 18 (2000) 420–432. doi:10.1016/S0167-7799(00)01474-8.

[15] V.B. Rewatkar, J.B. Joshi, Role of sparger design on gas dispersion in mechanically agitated gas-liquid contactors, Can. J. Chem. Eng. 71 (1993) 278–291. doi:10.1002/cjce.5450710215.

[16] F. Garcia-Ochoa, E. Gomez, Bioreactor scale-up and oxygen transfer rate in microbial processes: An overview, Biotechnol. Adv. 27 (2009) 153–176. doi:10.1016/j.biotechadv.2008.10.006.

[17] A. Morão, C.I. Maia, M.M.R. Fonseca, J.M.T. Vasconcelos, S.S. Alves, Effect of antifoam addition on gas-liquid mass transfer in stirred fermenters, Bioprocess Eng. 20 (1999) 165. doi:10.1007/s004490050576.

[18] C.M. Cooper, G.A. Fernstrom, S.A. Miller, Correction - Performance of Agitated Gas-Liquid Contactors, Ind. Eng. Chem. 36 (1944) 857–857. doi:10.1021/ie50417a601.

[19] B.H. Junker, Scale-up methodologies for Escherichia coli and yeast fermentation processes, J. Biosci. Bioeng. 97 (2004) 347–364. doi:10.1016/S1389-1723(04)70218-2.

[20] F. Scargiali, A. Busciglio, F. Grisafi, A. Brucato, Simplified dynamic pressure method for kLa measurement in aerated bioreactors, Biochem. Eng. J. 49 (2010) 165–172. doi:10.1016/j.bej.2009.12.008.

[21] M. Blažej, J. Annus, J. Markoš, Comparison of Gassing-out and Pressure-step Dynamic Methods for kLa Measurement in an Airlift Reactor with Internal Loop, Chem. Eng. Res. Des. 82 (2004) 1375–1382. doi:10.1205/cerd.82.10.1375.46737.

[22] O.S. Wolfbeis, Luminescent sensing and imaging of oxygen: Fierce competition to the Clark electrode, BioEssays. 37 (2015) 921–928. doi:10.1002/bies.201500002.

[23] P. Harms, Y. Kostov, G. Rao, Bioprocess monitoring., Curr. Opin. Biotechnol. 13 (2002) 124–7. doi:10.1016/S0958-1669(02)00295-1.

[24] R. Ramamoorthy, P.K. Dutta, S.A. Akbar, No Title, J. Mater. Sci. 38 (2003) 4271–4282. doi:10.1023/A:1026370729205.

[25] G. Ruchti, I.J. Dunn, J.R. Bourne, Comparison of dynamic oxygen electrode methods for the measurement of kLa, Biotechnol. Bioeng. 23 (1981) 277–290. doi:10.1002/bit.260230204.

[26] V. Gesellschaft, Druckverlust in durchströmten Rohren, in: VDI-Wärmeatlas, Springer, Berlin, Heidelberg, 2013: p. 1500. doi:10.1007/978-3-642-19981-3.

10.Appendices

10.1. Appendix A - Technical drawings

20L Laboratory Fermenter DIN A3

150L Glass reactor DIN A3

10.2. Appendix B - List of figures

10.3. Appendix C - List of Tables